CARDIAC

Diagnostic performance of quantitative, semi-quantitative, and visual analysis of dynamic CT myocardial perfusion imaging: a validation study with invasive fractional flow reserve

Yuehua Li[1] · Xu Dai[1] · Zhigang Lu[2] · Chengxing Shen[2] · Jiayin Zhang[1]

Abstract

Objectives To investigate the diagnostic performance of absolute myocardial blood flow (MBF), MBF_{ratio}, and visual analysis of dynamic CT myocardial perfusion imaging (CT-MPI) for the detection of hemodynamically significant coronary stenosis.

Methods Consecutive patients with chest pain and intermediate-to-high pre-test probability of obstructive coronary artery disease were prospectively enrolled. All patients were referred for dynamic CT-MPI and fractional flow reserve (FFR) measurements within 4 weeks. Absolute MBF, MBF_{ratio} (mean MBF of stenosis-subtended territories versus that of reference territories), and visually identified perfusion defect were tested for the diagnostic performance with reference to FFR.

Results Sixty-two patients with 95 target vessels were included for final analysis. The mean radiation dose for dynamic CT-MPI was 3.0 (2.2–4.0) mSv. The mean lesion-based absolute MBF value was significantly lower in ischemic segments than that in non-ischemic segments (78.0 (65.0–86.0) mL/min/100 mL vs. 133.0 (117.5–163.8) mL/min/100 mL, $p < 0.001$). Similarly, the lesion-based MBF_{ratio} was also markedly lower in territories with positive FFR results (0.52 (0.44–0.64) vs. 0.93 (0.91–0.97), $p < 0.001$). According to per-lesion ROC curve analysis, MBF and MBF_{ratio} had a similar area under the curve (AUC) for detecting hemodynamically significant lesions (AUC = 0.942 vs. 0.956, $p = 0.413$), which were larger than that of visual analysis (AUC = 0.802, both $p < 0.01$). The vessel-based sensitivity, specificity, and diagnostic accuracy were 84.3%, 97.7%, and 90.5% for MBF and 96.1%, 93.2%, and 94.7% for MBF_{ratio}.

Conclusions Absolute MBF and MBF_{ratio} had similarly excellent diagnostic performance with reference to FFR. In addition, these two parameters outperformed visual analysis for the detection of myocardial ischemia.

Key Points
• *The mean MBF and MBF_{ratio} were significantly lower in ischemic segments than those in non-ischemic segments.*
• *Absolute MBF and MBF_{ratio} had similar AUCs for the detection of hemodynamically significant lesions (AUC = 0.942 vs. 0.956, $p = 0.413$), which were larger than that of visual analysis (AUC = 0.802, both $p < 0.01$).*
• *The vessel-based sensitivity, specificity, and diagnostic accuracy were 84.3%, 97.7%, and 90.5% for absolute MBF and 96.1%, 93.2%, and 94.7% for MBF_{ratio}.*

Yuehua Li and Xu Dai contributed equally to this work.

Electronic supplementary material The online version of this article (https://doi.org/10.1007/s00330-020-07145-5) contains supplementary material, which is available to authorized users.

✉ Jiayin Zhang
  andrewssmu@msn.com

[1] Institute of Diagnostic and Interventional Radiology, Shanghai Jiao Tong University Affiliated Sixth People's Hospital, No. 600, Yishan Rd,, Shanghai 200233, China

[2] Department of Cardiology, Shanghai Jiao Tong University Affiliated Sixth People's Hospital, No. 600, Yishan Rd, Shanghai, China

Abbreviations

CAD   Coronary artery disease
CCTA   Coronary computed tomography angiography
CT   Computed tomography
FFR   Fractional flow reserve
ICA   Invasive coronary angiography
MBF   Myocardial blood flow
MPI   Myocardial perfusion imaging

Introduction

Diagnosis of coronary artery disease (CAD) requires not only anatomical but also functional evaluation in order to optimize the treatment strategy [1]. Coronary CT angiography (CCTA) has been validated as one non-invasive imaging modality that can accurately rule out obstructive CAD [2, 3]. However, this approach is unable to assess the hemodynamic significance of coronary stenosis, which is also essential for guiding treatment [4].

CT myocardial perfusion imaging (CT-MPI) combined with CCTA is an emerging technique that allows "one-stop shop" imaging of coronary vasculature as well as myocardial perfusion [5]. Static protocol is one CT-MPI acquisition method that provides only visual analysis of perfusion defect at lower radiation dose [6]. In contrast, dynamic CT-MPI enables absolute quantification and semi-quantification of various perfusion parameters at the cost of longer acquisition period and higher radiation exposure [7]. However, the diagnostic performance of these two approaches significantly varied between different studies with different methodologies [6–11] and no previous study has

made head-to-head comparison of diagnostic accuracy between quantitative, semi-quantitative, and visual analysis. At present, there is no consensus regarding the standardized approach for CT-MPI interpretation and it is of clinical importance to determine the optimal way for ischemia evaluation by intra-individual comparison of the aforementioned methods. Therefore, we aimed to investigate the diagnostic accuracy of quantitative, semi-quantitative, and visual analysis of dynamic CT-MPI with reference to invasive fractional flow reserve (FFR).

Materials and methods

Patient population

Between January 1, 2018, and December 31, 2019, we prospectively enrolled symptomatic patients with intermediate to high pre-test probability of obstructive CAD for dynamic CT-MPI + CCTA followed by invasive coronary angiography (ICA) + FFR measurement. The inclusion criteria were (1) patients with stable angina or angina-equivalent symptoms; and (2) the pre-test probability of obstructive CAD was intermediate to high according to updated Diamond-Forrester score (pre-test probability ≧ 15%). Exclusion criteria were (1) patients with previous history of coronary revascularization; (2) patients with previous history of myocardial infarction; (3) patients with suspected cardiomyopathy or microvascular dysfunction; (4) invasive FFR was not performed due to the absence of 40 to 90% stenosis on ICA; (5) image quality of dynamic CT-MPI was significantly impaired (Fig. 1).

Fig. 1 Flow chart of inclusion and exclusion. *Abbreviations*: CAD, coronary artery disease; CCTA, coronary computed tomography angiography; CT, computed tomography; FFR, fractional flow reserve; HCM, hypertrophic cardiomyopathy; ICA, invasive coronary angiography; MPI, myocardial perfusion imaging
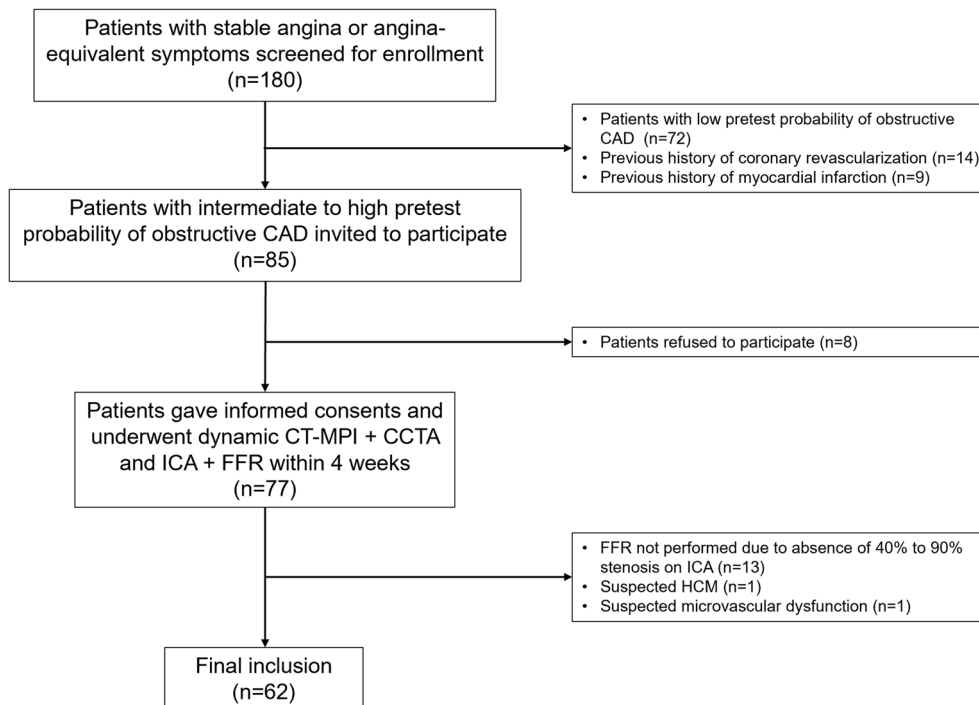
All recruited patients were referred for dynamic CT-MPI + CCTA followed by ICA + FFR measurement within 4-week interval regardless of the dynamic CT-MPI results. The hospital ethics committee approved this prospective study and the written informed consents were acquired from all participants.

Imaging protocol of dynamic CT-MPI

All patients were scanned with third-generation dual-source CT (SOMATOM Force, Siemens Healthineers), and an integrated protocol, which incorporated calcium score, dynamic CT-MPI, and CCTA, was employed. In brief, calcium score was firstly performed to calculate the calcification burden of each pericardial vessel. Intravenous infusion of adenosine triphosphate (ATP) at 160 μg/kg/min was then administrated for 3 min before the triggering of dynamic CT-MPI acquisition [12]. Dynamic CT-MPI was acquired using a shuttle mode technique and started 4 s after the beginning of contrast injection. Dynamic acquisition was set at the end-systolic phase (triggered at 250 ms after the R wave in all patients) and scans were launched every second or third heart cycle according to patients' heart rate. CARE kV and CARE dose 4D was used to reduce radiation dose. The reference tube voltage and effective current was 80 kVp and 300 mAs, respectively. Nitroglycerin was given sublingually in all subjects 5 min after dynamic CT-MPI. Prospective ECG-triggered sequential acquisition was performed in all participants for CCTA. The detailed parameters of contrast medium injection, dynamic CT-MPI, and CCTA acquisition were given in online appendix.

Image analysis of dynamic CT-MPI

Dataset of dynamic CT-MPI was reconstructed with a dedicated kernel (Qr36) for the reduction of iodine beam-hardening artifacts and analyzed using a commercially available CT-MPI software package (Myocardial perfusion analysis, VPCT body, Siemens Healthineers). Motion correction was manually applied if breathing-related misregistration of the left ventricle was present. The quantification of myocardial blood flow (MBF) was performed using a hybrid deconvolution model, as previously reported [13]. Image interpretation of CT-MPI was performed using different approaches as described below.

Visual analysis was made on three multiplanar-reformatted short-axis views (apical, mid, and basal) with 10-mm slice thickness. A narrow window width (200 HU) and window level (100 HU) was used for image interpretation [14]. Dynamic video data of the above short-axis views was visually evaluated frame by frame for detection of ischemic perfusion defect, which was defined as the hypo-density area that persisted throughout the cardiac cycle [14]. Any presence of ischemic perfusion defect was recorded according to 17-segment model [15] with the exclusion of the apical segment.

For absolute quantitative analysis, the region of interest (ROI) was manually placed on short-axis view to sample the MBF on a segment base according to the aforementioned 17-segment model with the exclusion of the apical segment. The ROI was drawn to cover the whole area of suspected perfusion defects within the segment or cover the whole segment when perfusion defect was absent. The stenosis-subtended territories and reference territories were each determined according to the fusion images of coronary vasculature and perfusion map. The mean value of stress MBF was measured for each segment of both stenosis-subtended territories and reference territories.

For semi-quantitative analysis, the stress MBF ratio (MBF_{ratio}) was adopted in the current study. This parameter was defined as the mean MBF of stenosis-subtended territories versus that of reference territories. In order to avoid underestimating the reference MBF, the reference territories were defined as all the myocardial segments supplied by epicardial vessels without the presence of ≥ 30% stenosis, of which the hemodynamic status was considered insignificant [16].

Two cardiovascular radiologists (with 10 years and 6 years of experience in cardiovascular imaging), who were blinded to clinical histories, independently analyzed all CT-MPI data. Any disagreement regarding qualitative analysis was resolved by consensus. The mean values of quantitative parameters measured by two observers were used for analysis.

Image analysis of CCTA

Axial images were reconstructed with smooth kernel (Bv 40) and third-generation iterative reconstruction (IR) technique (strength 3, ADMIRE, Siemens). Data were transferred to an offline workstation (SyngoVia VB10, Siemens Healthineers) and the dataset with the best image quality throughout available cardiac phases was used for further evaluation.

Diameter stenosis (DS) was semi-automatically quantified as (reference diameter – minimal lumen diameter) / reference diameter. Two cardiovascular radiologists (with 10 years and 6 years of experience in cardiovascular imaging), who were blinded to clinical histories and CT-MPI results, independently analyzed the lesions and the mean values of DS measured by two observers were used for further analysis.

ICA and FFR measurement

ICA was performed by two interventional cardiologists (with 26 years and 20 years' experience of coronary intervention) with standard method and at least two views were obtained for each major vessel. The stenotic extent of each lesion was visually assessed without the knowledge of dynamic CT-

MPI and CCTA results. Invasive FFR was measured by using a 0.014-in. pressure guidewire (Abbott) as previously described [4]. Hyperemia was induced by intravenous infusion of ATP at 160 μg/kg/min. FFR measurement was performed in all lesions on major coronary arteries (caliber $\geqq$ 2.5 mm) with stenosis severity between 40 and 90% [17]. An FFR value of ≤ 0.8 was considered physiologically significant stenosis.

Comparison of CT-MPI and invasive FFR

For the prespecified reference standard, all vessels interrogated with invasive FFR were classified into ischemic and non-ischemic according to FFR results. Vessels having any lesion with FFR ≤ 0.8 were defined as ischemic whereas vessels not having any lesion with FFR ≤ 0.8 were defined as non-ischemic.

Comparison of multiple qualitative, quantitative, and semi-quantitative CT-derived parameters with the reference standard was made on a vessel-based analysis and patient-based analysis. For CT-quantified DS, the lesions with the most severe stenosis extent on one specific vessel were selected for comparison with invasive FFR (in case of the presence of tandem lesions). For visual analysis of CT-MPI, vessels with the presence of any visible perfusion defect within the territories were considered ischemic and further compared with FFR results. For quantitative and semi-quantitative analysis, the best cutoff values derived from receiver operating characteristic (ROC) analyses were used to distinguish ischemic and non-ischemic vessels.

Statistical analysis

Statistical analysis was performed by using commercial statistical software (MedCalc Statistical Software version 15.2.2, MedCalc Software bvba). One-sample Kolmogorov-Smirnov test was used to check the assumption of normal distribution. Normally distributed continuous quantitative variables were expressed as means ± standard deviations, or median with first to third quartile otherwise. Student's t test was used for normally distributed data, and the Mann-Whitney U test was used for data that were not normally distributed. The average measures for intra-observer and inter-observer agreements were expressed in intra-class correlation coefficient (ICC) and Cohen's kappa coefficient when data were continuous variables and categorical variables respectively. The relationship between invasive FFR, MBF, and MBF$_{ratio}$ was assessed by the Pearson correlation analysis. ROC curve analyses were performed to calculate the area under the receiver operating characteristic curve (AUC). The optimal cutoff values for various parameters were determined by the Youden index, the maximum sum of sensitivity and specificity. Diagnostic performance was compared using ROC

analysis with DeLong's method. Sensitivity, specificity, positive predictive value (PPV), negative predictive value (NPV), and accuracy were recorded. The sensitivity, specificity, and diagnostic accuracy between visual analysis, MBF, and MBF$_{ratio}$ were compared using the McNemar test. A two-tailed $p < 0.05$ was considered statistically significant.

Results

Clinical demographics of study participants

Between January 1, 2018, and December 31, 2019, consecutive 180 patients with angina or angina-equivalent symptoms were clinically evaluated in cardiology service and those with intermediate-to-high pre-test probability of obstructive CAD were screened for recruitment. Seventy-two patients were initially excluded because of low pre-test probability of obstructive CAD whereas 25 patients were excluded due to the clinical history of myocardial infarction or revascularization. Eight patients who refused to provide informed consent were also excluded. After the enrollment, fifteen patients were further excluded due to various reasons as shown in Fig. 1.

Sixty-two patients (mean age, 65 ± 10 [range, 46–83] years; 54 men (mean age, 65 ± 10 [range, 46–82] years) and 8 women (mean age, 67 ± 9 [range 51–83] years; $p = 0.339$) with 95 vessels interrogated by FFR were finally included in the present study. The dose length product of dynamic CT-MPI and the whole integrated CT protocol (scout view, calcium score, dynamic CT-MPI, and CCTA) were 211.7 (160.2–284.8) mGy*cm and 385.5 (336.5–543.0) mGy*cm respectively. The mean effective doses of radiation for dynamic CT-MPI and the whole integrated CT protocol were 3.0 (2.2–4.0) mSv and 5.4 (4.7–7.6) mSv respectively when using 0.014 as the conversion factor. The mean interval between CT examinations and invasive tests was 13.9 ± 9.8 days (range 1 to 30 days). The mean time for dynamic CT-MPI post-processing and image analysis was 25.8 ± 4.2 min (19–37 min). Other clinical details were given in Table 1.

Characteristics of CT-derived imaging parameters between ischemic and non-ischemic lesions

The intra-observer and inter-observer agreement for the measurement of CT-derived parameters were good (online supplement Table E1 and E2). The mean lesion-based absolute MBF value was significantly lower in ischemic segments than that in non-ischemic segments (78.0 (65.0–86.0) mL/min/100 mL vs. 133.0 (117.5–163.8) mL/min/100 mL, $p < 0.001$). Similarly, the lesion-based MBF$_{ratio}$ was also markedly lower in territories with positive FFR results (0.52 (0.44–0.64) vs. 0.93 (0.91–0.97), $p < 0.001$). In addition, for ischemic vessel territories, the visible perfusion defect was

Table 1 Demographic data

Baseline characteristics	Total ($n = 62$)
Age (years)	65.0 ± 10.1
Male (%)	54 (87.1)
BMI[*]	24.95 ± 3.06
Risk factors	
Diabetes mellitus (%)	28 (45.2)
Hypertension (%)	54 (87.1)
Dyslipidemia (%)	27 (43.5)
Current smoking (%)	32 (51.6)
CACS[†]	110.85 (21.53–291.10)
Pre-test probability (%)[‡]	
15–65%	12 (19.4)
66–85%	32 (51.6)
>85%	18 (29)
HR (bpm) [*]	
Baseline	70.0 ± 10.1
Stress	84.4 ± 12.3
CM volume (mL) [*]	97.4 ± 5.5
Radiation dose (mSv) [†]	
Total CT protocol	5.4 (4.7–7.6)
Dynamic CT-MPI	3.0 (2.2–4.0)
Interval between CT and ICA (days) [*]	13.87 ± 9.77
Subsequent treatment	
PCI (%)	39 (62.9)
Medical (%)	23 (37.1)

[*]Data are means ± standard deviations

[†] Data are the median, with the interquartile range in parentheses

[‡] Calculated by using the Diamond and Forrester Chest Pain Prediction Rule

Abbreviations: *BMI* body mass index, *CACS* Coronary Artery Calcium Scoring, *CM* contrast medium, *FFR* fractional flow reserve, *HR* heart rate, *PCI* percutaneous coronary intervention

more frequently presented whereas CT-quantified DS was significantly higher (Table 2). Representative cases showing ischemic and non-ischemic lesions were given in Figs. 2 and 3. According to correlation analysis, both lesion-based MBF and MBF$_{ratio}$ correlated well with FFR results (Fig. 4).

Diagnostic performance of visual analysis, absolute quantification, and semi-quantification of dynamic CT-MPI for predicting hemodynamically significant stenosis

As for lesion-based evaluation, 51 vessels were diagnosed by FFR as functionally significant lesions. According to ROC analysis, absolute MBF and MBF$_{ratio}$ had similarly large AUC on per-vessel level (AUC = 0.942 vs. AUC = 0.956, $p = 0.413$). In contrast, the visual analysis resulted in smaller AUC compared with quantitative and semi-quantitative assessment (Fig. 5). When using 89.5 mL/min/100 mL and 0.81 as the best cutoffs, the overall diagnostic accuracies of MBF and MBF$_{ratio}$ were 90.5% (86/95) and 94.7% (90/95) respectively on a per-vessel level. Visual analysis (78.9%, compared with MBF and MBF ratio, $p = 0.007$ and $p < 0.001$ respectively) and CT-quantified DS (72.6%, compared with MBF and MBF ratio, $p = 0.005$ and $p = 0.001$ respectively) were shown to have inferior diagnostic accuracy compared with the two aforementioned parameters (Table 3).

As for patient-based analysis, similar results were also observed as absolute MBF and MBF$_{ratio}$ had the highest diagnostic accuracy, sensitivity, specificity, PPV, and NPV compared to visual interpretation and CT-quantified DS. The AUCs of MBF and absolute MBF and MBF$_{ratio}$ on a per-patient level were 0.977 and 0.972 respectively. Details were given in Table 3. In addition, for male patients, the AUCs of MBF visual, absolute MBF, and MBF$_{ratio}$ were 0.833, 0.991, and 0.995 respectively (all $p < 0.001$), which were similar to those for total population. According to MBF$_{ratio}$ analysis, 21 patients in the current cohort had negative perfusion result and would have been deferred from further invasive tests.

Discussion

The major finding of the current study was that the absolute MBF and MBF$_{ratio}$ had similarly excellent diagnostic performance with reference to invasive FFR. In addition, quantitative and semi-quantitative evaluation outperformed visual analysis for the detection of myocardial ischemia.
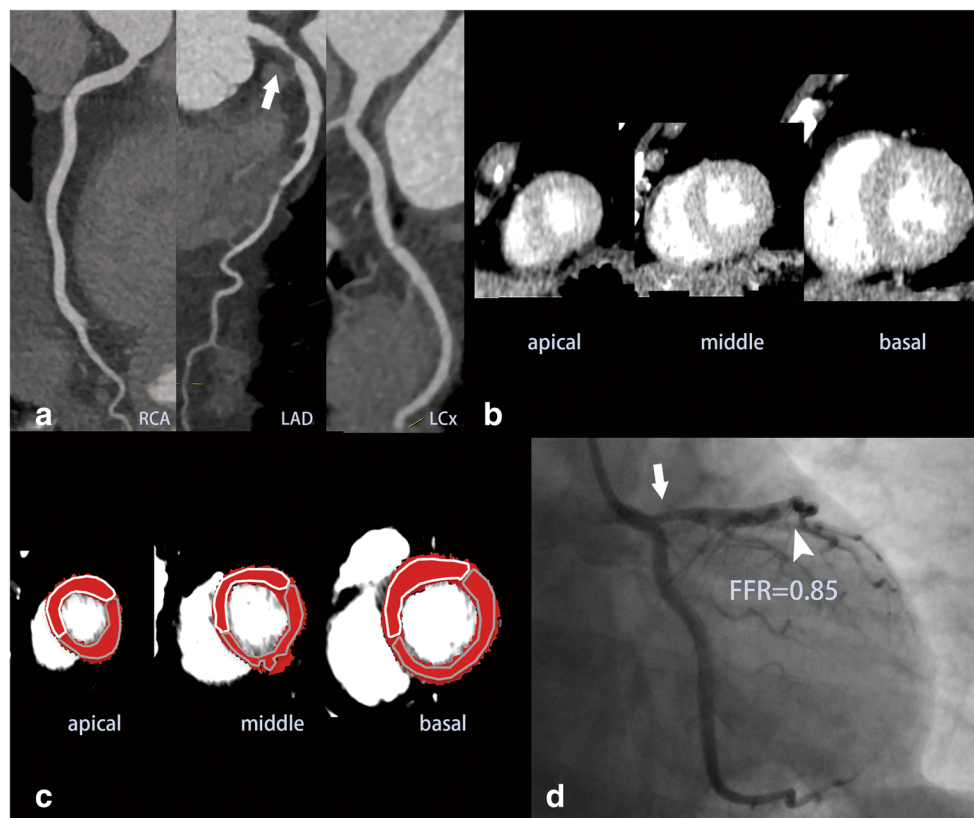
Table 2 Characteristics of CT-derived imaging parameters between ischemic and non-ischemic lesions

	Total ($n = 95$)	FFR ≤ 0.8 ($n = 51$)	FFR > 0.8 ($n = 44$)	p
Diameter stenosis (%)	68.9 ± 13.7	75.6 ± 10.2	61.0 ± 13.2	< 0.001
Perfusion defect by visual analysis (%)	33 (34.7)	32 (62.7)	1 (2.3)	< 0.001
MBF (mL/min/100 mL)	94.0 (78.0–134.0)	78.0 (65.0–86.0)	133.0 (117.5–163.8)	< 0.001
MBF $_{ratio}$	0.73 (0.52–0.94)	0.52 (0.44–0.64)	0.93 (0.91–0.97)	< 0.001

Abbreviations: *CT* computed tomography, *FFR* fractional flow reserve, *MBF* myocardial blood flow

Fig. 2 Representative case of a 51-year-old female presenting with atypical chest pain. Dynamic CT-MPI provided functional information to accurately exclude myocardial ischemia of severe stenosis. **a** CPR images showed non-calcified plaque at LAD ostium with severe stenosis (white arrow) whereas the other two major coronary arteries were free of stenosis. **b** Short-axis views (from apical to basal) of visual analysis did not reveal perfusion defect in any segment. **c** Short-axis views (from apical to basal) of MBF color-coded map demonstrated the absence of decreased perfusion. The mean MBF of LAD territory (white area) was 223 mL/min/100 mL and mean MBF of reference segments (gray area) was 218 mL/min/100 mL. The MBF$_{ratio}$ was 1.02 accordingly. **d** ICA confirmed the severe stenosis at LAD ostium (white arrow). FFR was measured as 0.85 for this lesion (white arrowhead). *Abbreviations*: CPR, curved planar reformation; CT, computed tomography; FFR, fractional flow reserve; ICA, invasive coronary angiography; LAD, left anterior descending; MBF, myocardial blood flow; MPI, myocardial perfusion imaging

The integrated CT-MPI and CCTA scan allow one-stop-shop imaging for functional and anatomical evaluation of obstructive CAD. In contrast to static perfusion imaging protocol, dynamic CT-MPI enables absolute calculation of MBF for ischemia assessment, which can theoretically enhance the detection of myocardial ischemia. According to the present finding, absolute MBF was able to discriminate flow-limiting from non-flow-limiting coronary stenosis at high sensitivity (84.3%, 43/51) and specificity (97.7%, 43/44). The diagnostic accuracy of MBF in the current study was better than those reported in previous studies [18–20], which can be mainly explained by the technical development of CT scanners. The present study employed third-generation dual-source CT, which allowed dynamic CT-MPI acquisition at higher temporal resolution (66 ms) and with less motion artifact compared with other CT scanners. In addition, the use of a dedicated reconstruction kernel (Qr36) could further reduce beam hardening artifact and led to better quantification accuracy. However, it is also notable that the best cutoff of MBF for discriminating ischemic and non-ischemic varied from 75 mL/min/100 mL to 113 mL/min/100 mL according to different previous studies [9, 18–21]. Various factors may affect the individual stress hyperemic extent and different calculation algorithms also lead to discrepant MBF results [22]. Therefore, it is conceivable that using one single absolute MBF value to diagnose myocardial ischemia in different cohorts is challenging.

In addition to absolute quantification, the current study also found that MBF$_{ratio}$ had similarly high diagnostic accuracy compared with MBF. When using 0.81 as the best cutoff value, MBF$_{ratio}$ was able to accurately differentiate functionally significant and insignificant stenosis in 94.7% (90/95) of total lesions. According to the definition of MBF$_{ratio}$, 0.81 corresponds to a roughly 20% decrease of myocardial perfusion compared with the reference segments. It is interesting to note that this value is very close to the percentage of pressure drop used by invasive FFR to diagnose hemodynamically significant lesions. In cases without microvascular dysfunction, the extent of reduced myocardial perfusion is theoretically similar to the percentage of pressure drop across coronary
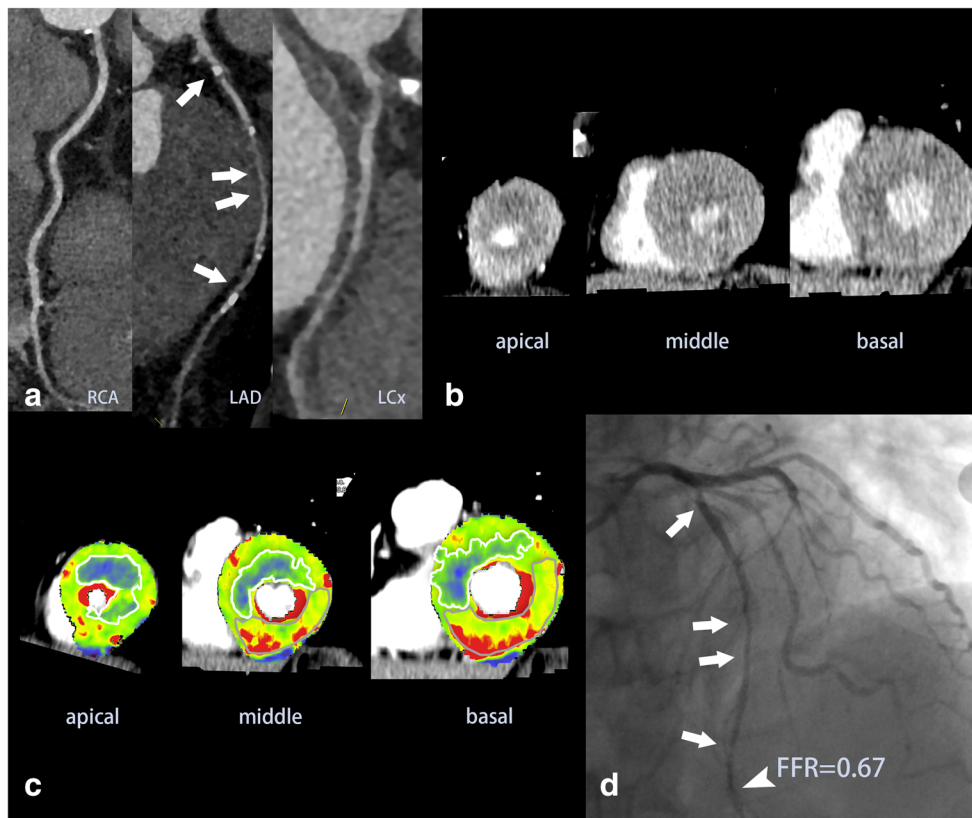
Fig. 3 Representative case of a 69-year-old male presenting with exertional chest pain. Dynamic CT-MPI provided functional information to accurately diagnose myocardial ischemia of moderate stenosis. **a** CPR images showed calcified and mixed plaques at proximal to middle LAD with multiple moderate stenosis (white arrow) whereas other two major coronary arteries were with lumen irregularity and minimal stenosis. **b** Short-axis views (from apical to basal) of visual analysis revealed diffuse perfusion defect in anterior and septal wall. **c** Short-axis views (from apical to basal) of MBF color-coded map demonstrated the extensive reduced myocardial perfusion in anterior, septal wall as well as part of lateral wall. The mean MBF of LAD territory (white area) was 62 mL/min/100 mL and mean MBF of reference segments (gray area) was 138 mL/min/100 mL. The MBF$_{ratio}$ was 0.45 accordingly. Please note that the area with decreased MBF was slightly larger than that with perfusion defect by visual analysis. **d** ICA confirmed the diffuse moderate stenosis at proximal to middle LAD (white arrow). FFR was measured as 0.67 for this lesion (white arrowhead). *Abbreviations*: CPR, curved planar reformation; CT, computed tomography; FFR, fractional flow reserve; ICA, invasive coronary angiography; LAD, left anterior descending; MBF, myocardial blood flow; MPI, myocardial perfusion imaging

stenosis. Moreover, unlike absolute MBF value which can be affected by various factors, MBF$_{ratio}$ represents the relative MBF reduction of stenosis-subtended territory with comparison to reference territory. We consequently hypothesized that
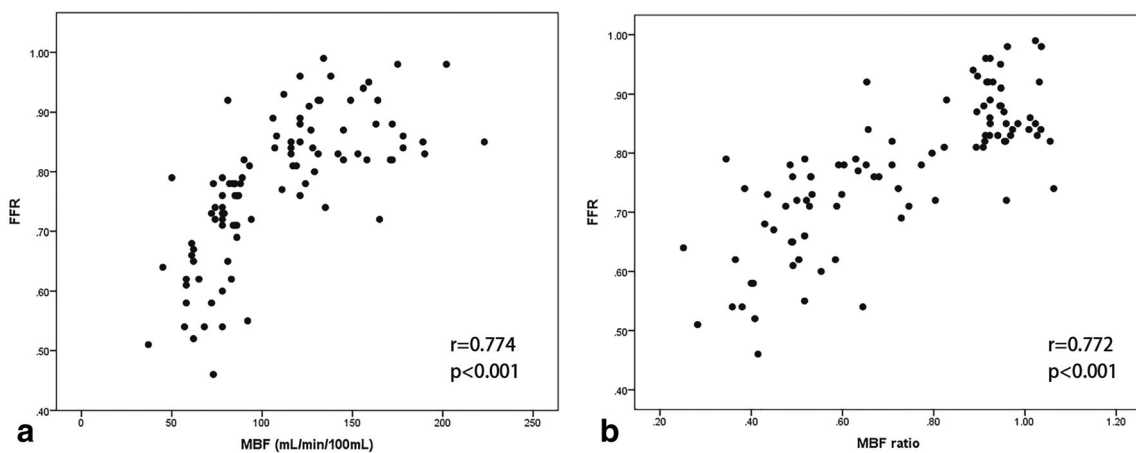

Fig. 4 Pearson correlation analysis of MFB and MBF$_{ratio}$ versus invasive FFR measurement. MBF (**a**) and MBF$_{ratio}$ (**b**) correlated well with invasive FFR measurement. *Abbreviations*: FFR, fractional flow reserve; MBF, myocardial blood flow
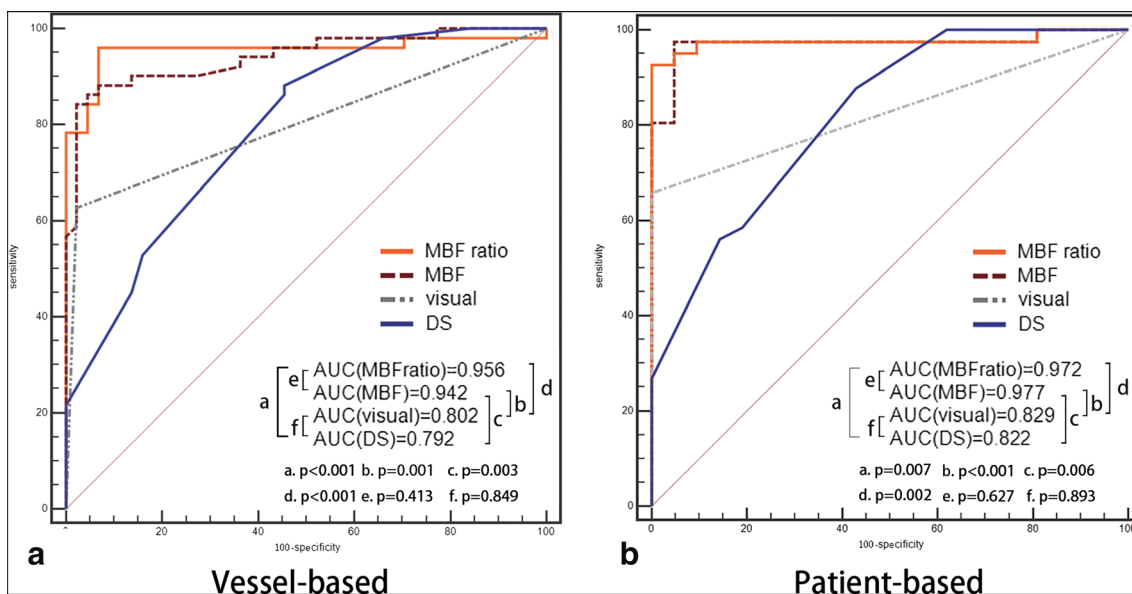
Fig. 5 ROC curve analysis of dynamic CT-MPI for identifying functionally significant coronary stenosis. Vessel-based (**a**) and patient-based (**b**) analysis showing that MBF and MBF_ratio had significantly larger AUC compared with visual analysis and DS. *Abbreviations*:

AUC, area under the curve; CT, computed tomography; DS, diameter stenosis; FFR, fractional flow reserve; MBF, myocardial blood flow; MPI, myocardial perfusion imaging

this ratio will be highly reproducible even in a more generalized population regardless of the MBF calculation algorithm. Thus, MBF_ratio might be a more robust parameter than absolute MBF for dynamic CT-MPI interpretation in real-world clinical practice.

Moreover, the current study also investigated the diagnostic performance of visual analysis of dynamic CT-MPI. According to the present findings, perfusion defect by visual analysis had high specificity (97.7%, 43/44) but low

sensitivity (62.7%, 32/51) and the overall diagnostic accuracy was lower than those of MBF and MBF_ratio. The underlying reason for this inferiority can be explained by the insufficient attenuation difference to be detected by visual analysis between ischemic and non-ischemic segments, especially for lesions with mild ischemia and small area of involvement. This finding suggests that visual analysis should not be adopted as the main evaluation approach when quantitative analysis is available. Also, static CT-MPI, which only allows

Table 3 Diagnostic performance of CT-derived imaging parameters for predicting hemodynamically significant stenosis

	AUC	Cutoff value	Sensitivity (%)	Specificity (%)	PPV (%)	NPV (%)	Accuracy (%)
Vessel-based analysis (n = 95)							
Diameter stenosis (%)	0.792	62.5	88.2% (45/51)	54.5% (24/44)	69.2% (45/65)	80.0% (24/30)	72.6% (69/95)
Perfusion defect by visual analysis	0.802	–	62.7% (32/51)	97.7% (43/44)	97.0% (32/33)	69.4% (43/62)	78.9% (75/95)
Diameter stenosis combined with perfusion defect by visual analysis*	0.802	–	62.7% (32/51)	97.7% (43/44)	97.0% (32/33)	69.4% (43/62)	78.9% (75/95)
MBF (mL/min/100 mL)	0.942	89.5	84.3% (43/51)	97.7% (43/44)	97.7% (43/44)	84.3% (43/51)	90.5% (86/95)
MBF_ratio	0.956	0.81	96.1% (49/51)	93.2% (41/44)	94.2% (49/52)	95.3% (41/43)	94.7% (90/95)
Patient-based analysis (n = 62)							
Diameter stenosis (%)	0.822	65.0	87.8% (36/41)	57.1% (12/21)	80.0% (36/45)	70.6% (12/17)	77.4% (48/62)
Perfusion defect by visual analysis	0.829	–	65.9% (27/41)	100% (21/21)	100% (27/27)	60.0% (21/35)	77.4% (48/62)
Diameter stenosis combined with perfusion defect by visual analysis*	0.829	–	65.9% (27/41)	100% (21/21)	100% (27/27)	60.0% (21/35)	77.4% (48/62)
MBF (mL/min/100 mL)	0.977	92.5	92.7% (38/41)	100% (21/21)	100% (38/38)	87.5% (21/24)	95.2% (59/62)
MBF_ratio	0.972	0.81	97.6% (40/41)	95.2% (20/21)	97.6% (40/41)	95.2% (20/21)	96.8% (60/62)

*Lesions were considered hemodynamically significant when CCTA showed ≥ 50% and visual analysis of CT-MPI revealed visible perfusion defect

Abbreviations: *AUC* area under the curve, *CCTA* coronary computed tomography angiography, *CT* computed tomography, *MBF* myocardial blood flow, *NPV* negative predictive value, *PPV* positive predictive value

visual analysis for assessment, should be replaced by dynamic CT-MPI if the latter one is technically feasible on the in-use CT scanners.

As for other non-invasive imaging modalities for ischemia evaluation, CT fractional flow reserve (CT-FFR) and magnetic resonance myocardial perfusion imaging (MR-MPI) are two alternatives to dynamic CT-MPI. CT-FFR has the advantage of having no additional radiation exposure and less contrast medium consumption compared with CT-MPI [23]. However, impaired image quality of CCTA and heavy calcification may negatively affect the diagnostic performance of CT-FFR [24, 25]. According to one head-to-head comparison study, the diagnostic accuracy dynamic CT-MPI outperforms machine learning–based CT-FFR technique with reference to invasive FFR [9]. Other than CT-based approaches, MR-MPI is one more widely applied method in terms of ischemia assessment. With the latest technical development of cardiac magnetic resonance imaging, MR-MPI also enables absolute quantification of MBF without radiation burden and can accurately differentiate ischemic from non-ischemic lesions with reference to invasive FFR [26]. However, a direct comparison between CT-MPI and MR-MPI on the latest hardware platform is still absent and future studies are warranted to determine which modality is superior with regard to ischemia imaging.

Despite of the above promising findings, the present study has several limitations. First, the overall pre-test probability of obstructive CAD was high in the current cohort. The best cutoff values of MBF and MBF_{ratio} were generated from relatively high-risk patients. Therefore, these criteria still need to be validated in future studies with more low-to-intermediate risk patients. Second, all patients were scanned with third-generation dual-source CT in the current study. Although MBF_{ratio} might not be affected, the results of absolute MBF and visual analysis could be altered if different hardware and calculation algorithm are employed. Thus, future investigation is also warranted to confirm those results on different CT scanners. Third, the majority of included patients (87.1%) were males and therefore gender-based sub-analysis was not feasible. Symptomatic female patients are more likely to suffer from microvascular dysfunction, which could be a diagnostic challenge for CT-MPI [27]. So the present results may not be applied to the symptomatic patients with microvascular dysfunction. Finally, the measurement of MBF was performed manually with non-fixed ROIs according to the actual area with decreased MBF. This method is semi-automated rather than fully automated and requires long postprocessing/image analysis time (mean time, 25.8 ± 4.2 min). Future automated methods are needed to be developed to reduce the analyzing time.

In conclusion, the absolute MBF and MBF_{ratio} had similarly excellent diagnostic performance with reference to invasive FFR. In addition, quantitative and semi-quantitative evaluation outperformed visual analysis for the detection of myocardial ischemia.

Compliance with ethical standards

Guarantor The scientific guarantor of this publication is Dr. Jiayin Zhang.

Conflict of interest The authors of this manuscript declare no relationships with any companies whose products or services may be related to the subject matter of the article.

Statistics and biometry No complex statistical methods were necessary for this paper.

Informed consent Written informed consent was waived by hospital IRB.

Ethical approval Institutional Review Board approval was obtained.

Methodology
• prospective
• comparative study
• performed at one institution

References

1. Knuuti J, Wijns W, Saraste A et al (2020) 2019 ESC Guidelines for the diagnosis and management of chronic coronary syndromes. Eur Heart J 41(3):407–477
2. Miller JM, Rochitte CE, Dewey M et al (2008) Diagnostic performance of coronary angiography by 64-row CT. N Engl J Med 359(22):2324–2336
3. Westwood ME, Raatz HD, Misso K et al (2013) Systematic review of the accuracy of dual-source cardiac CT for detection of arterial stenosis in difficult to image patient groups. Radiology 267(2):387–395
4. Pijls NH, De Bruyne B, Peels K et al (1996) Measurement of fractional flow reserve to assess the functional severity of coronary-artery stenoses. N Engl J Med 334(26):1703–1708
5. Rossi A, Merkus D, Klotz E, Mollet N, de Feyter PJ, Krestin GP (2014) Stress myocardial perfusion: imaging with multidetector CT. Radiology 270:25–46
6. Ko BS, Cameron JD, Meredith IT et al (2012) Computed tomography stress myocardial perfusion imaging in patients considered for revascularization: a comparison with fractional flow reserve. Eur Heart J 33(1):67–77
7. Bamberg F, Marcus RP, Becker A et al (2014) Dynamic myocardial CT perfusion imaging for evaluation of myocardial ischemia as determined by MR imaging. JACC Cardiovasc Imaging 7(3):267–277
8. Coenen A, Rossi A, Lubbers MM et al (2017) Integrating CT myocardial perfusion and CT-FFR in the work-up of coronary artery disease. JACC Cardiovasc Imaging 10(7):760–770

9. Li Y, Yu M, Dai X et al (2019) Detection of hemodynamically significant coronary stenosis: CT myocardial perfusion versus machine learning CT fractional flow reserve. Radiology 293(2):305–314

10. Pontone G, Andreini D, Guaricci AI et al (2019) Incremental diagnostic value of stress computed tomography myocardial perfusion with whole-heart coverage CT scanner in intermediate- to high-risk symptomatic patients suspected of coronary artery disease. JACC Cardiovasc Imaging 12(2):338–349

11. Yi Y, Xu C, Wu W et al (2019) Myocardial blood flow analysis of stress dynamic myocardial CT perfusion for hemodynamically significant coronary artery disease diagnosis: the clinical value of relative parameter optimization. J Cardiovasc Comput Tomogr. https://doi.org/10.1016/j.jcct.2019.10.001

12. García-Baizán A, Millor M, Bartolomé P et al (2019) Adenosine triphosphate (ATP) and adenosine cause similar vasodilator effect in patients undergoing stress perfusion cardiac magnetic resonance imaging. Int J Cardiovasc Imaging 35(4):675–682

13. Bamberg F, Klotz E, Flohr T et al (2010) Dynamic myocardial stress perfusion imaging using fast dual-source CT with alternating table positions: initial experience. Eur Radiol 20:1168–1173

14. Yang DH, Kim YH, Roh JH et al (2015) Stress myocardial perfusion CT in patients suspected of having coronary artery disease: visual and quantitative analysis-validation by using fractional flow reserve. Radiology 276(3):715–723

15. Cerqueira MD, Weissman NJ, Dilsizian V et al (2002) Standardized myocardial segmentation and nomenclature for tomographic imaging of the heart: a statement for healthcare professionals from the Cardiac Imaging Committee of the Council on Clinical Cardiology of the American Heart Association. Circulation 105(4):5392542

16. Tonino PA, Fearon WF, De Bruyne B et al (2010) Angiographic versus functional severity of coronary artery stenoses in the FAME study fractional flow reserve versus angiography in multivessel evaluation. J Am Coll Cardiol 55(25):2816–2821

17. Nagel E, Greenwood JP, McCann GP et al (2019) Magnetic resonance perfusion or fractional flow reserve in coronary disease. N Engl J Med 380(25):2418–2428

18. Bamberg F, Becker A, Schwarz F et al (2011) Detection of hemodynamically significant coronary artery stenosis: incremental diagnostic value of dynamic CT-based myocardial perfusion imaging. Radiology 260:689–698

19. Rossi A, Wragg A, Klotz E et al (2017) Dynamic computed tomography myocardial perfusion imaging: comparison of clinical analysis methods for the detection of vessel-specific ischemia. Circ Cardiovasc Imaging 10(4):e005505

20. Yang J, Dou G, He B et al (2019) Stress myocardial blood flow ratio by dynamic CT perfusion identifies Hemodynamically significant CAD. JACC Cardiovasc Imaging. https://doi.org/10.1016/j.jcmg.2019.06.016

21. Pontone G, Baggiano A, Andreini D et al (2019) Dynamic stress computed tomography perfusion with a whole-heart coverage scanner in addition to coronary computed tomography angiography and fractional flow reserve computed tomography derived. JACC Cardiovasc Imaging 12(12):2460–2471

22. van Assen M, Pelgrim GJ, De Cecco CN et al (2019) Intermodel disagreement of myocardial blood flow estimation from dynamic CT perfusion imaging. Eur J Radiol 110:175–180

23. Yu M, Lu Z, Shen C et al (2019) The best predictor of ischemic coronary stenosis: subtended myocardial volume, machine learning-based FFR$_{CT}$, or high-risk plaque features? Eur Radiol 29(7):3647–3657

24. Yu M, Lu Z, Li W, Wei M, Yan J, Zhang J (2018) CT morphological index provides incremental value to machine learning based CT-FFR for predicting hemodynamically significant coronary stenosis. Int J Cardiol 265:256–261

25. Zhuang B, Wang S, Zhao S, Lu M (2020) Computed tomography angiography-derived fractional flow reserve (CT-FFR) for the detection of myocardial ischemia with invasive fractional flow reserve as reference: systematic review and meta-analysis. Eur Radiol 30(2):712–725

26. Kotecha T, Martinez-Naharro A, Boldrini M et al (2019) Automated pixel-wise quantitative myocardial perfusion mapping by CMR to detect obstructive coronary artery disease and coronary microvascular dysfunction: validation against invasive coronary physiology. JACC Cardiovasc Imaging 12(10):1958–1969

27. Feher A, Sinusas AJ (2017) Quantitative assessment of coronary microvascular function: dynamic single-photon emission computed tomography, positron emission tomography, ultrasound, computed tomography, and magnetic resonance imaging. Circ Cardiovasc Imaging 10(8):e006427